Immune dysfunction revealed by digital spatial profiling of immuno-oncology markers in progressively advanced stages of renal cell carcinoma, including brain metastases

David Schoenfeld[1], Myrto Moutafi[2], Sandra Martinez[2], Adebowale Adeniran[2], Lucia Jilaveanu[1], Michael Hurwitz[1], David L. Rimm[2], Wei Wei[3], Harriet Kluger[1]

[1]Section of Medical Oncology, Yale School of Medicine, New Haven, Connecticut, USA.[2] Department of Pathology, Yale School of Medicine, New Haven, Connecticut, USA. [3] Department of Biostatistics, Yale School of Public Health, New Haven, Connecticut, USA.

Abstract

Background:
The tumor immune microenvironment (TME) is an important contributor to cancer progression and response to therapy, including in renal cell carcinoma (RCC). Prior studies have investigated the TME in RCC, including using single-cell transcriptomics. However, these studies often include limited sample sizes and lack spatial orientation. One method to overcome some of these limitations involves digital spatial profiling (DSP), which allows for the quantitative assessment of multiplexed proteins or RNAs using oligonucleotide tags while preserving spatial orientation. DSP can be performed on formalin-fixed, paraffin-embedded tissue sections, enabling a high-throughput workflow and the use of archived samples. Specific cellular-molecular compartments, such as certain tissue or immune populations, can be interrogated separately using fluorescent markers. In this study, we aim to further characterize the TME of progressively advanced stages of RCC, including brain metastases, using DSP.

Methods:
We performed DSP on a GeoMx DSP instrument (NanoString Technologies) using a panel of 52 validated immuno-oncology markers, as well as three housekeeping proteins and three negative controls. We divided each specimen into cellular-molecular compartments based on fluorescence patterns with the following collection hierarchy: macrophage compartment (CD68+); leukocyte compartment (CD68-CD45+); and tumor/kidney compartment (pan-cytokeratin+). We profiled three different RCC tissue microarrays (TMAs), consisting of: 1) 25 matched adjacent normal kidney and primary RCC cases (YTMA-84); 2) 14 matched primary and metastatic RCC cases (YTMA-166); and 3) 95 tumor specimens from 59 unique patients with brain metastases, with 24 matched primary tumor and metastases pairs, with 25% of the TMA spots consisting of brain metastases specimens (YTMA-528). More than one tumor core or "replicate" was profiled for >70% of the tumor specimens from the second and third TMAs. Data were analyzed using a mixed-effects model with false-discovery rate correction for multiple comparisons. Univariate and multivariate Cox proportional hazards regression analyses of survival were also performed on the data from YTMA-528 based on an extensive clinical database that was constructed.

Results:
Compared to adjacent normal kidney, primary tumor samples were more infiltrated with macrophages and had higher levels of B7-H3, a B7 ligand family member with protumorigenic effects (in the macrophage and leukocyte compartments). In the tumor/kidney compartment, adjacent normal kidney had higher levels of p53 and the apoptotic proteins BAD and BIM. In both TMAs with matched primary and metastatic tumor specimens, expression of the immune checkpoints TIM-3, CTLA-4, and LAG3, as well as markers of T cell activation, GMZA, GZMB, and CD25, was lower in the leukocyte compartment of metastatic samples. In the macrophage compartment, expression of M1-like macrophage markers HLA-DR and CD127 was also lower in metastatic samples compared to primary tumors. Comparison of brain metastases to metastases from other anatomic locations revealed higher levels of the anti-apoptotic, BCL-2-family protein BCL-XL in all cellular compartments in brain metastases, and lower levels of STING. Multivariate Cox proportional hazards regression analysis revealed STING expression in leukocytes of primary tumors, but not metastases, as a potential prognostic marker for survival after brain metastasis occurrence.

Conclusions:
DSP of progressively advanced stages of RCC, including brain metastases, revealed reduced levels of multiple immune checkpoints and T cell activation markers in metastases versus primary tumor samples, and higher inflammatory macrophage activation markers in primary samples. As predictive biomarkers are developed for immunotherapy in RCC, care should be taken to sample tissue from the site requiring systemic therapy. Brain metastases also had features unique from metastases to other sites. These distinct TME features may have important implications for the design of future biomarker and treatment studies. Further validation is needed of potential prognostic and predictive markers.

Methods

Figure 1: DSP steps

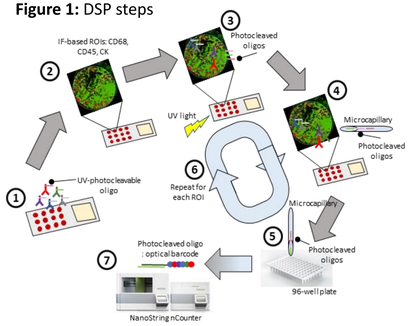

adapted from Kulasinghe et al, *Front Oncol*, 2021.

Figure 1. DSP steps: (1)TMA slides were incubated with a panel of photocleavable oligonucleotide-conjugated antibodies validated by NanoString and directed towards 52 immuno-oncology markers, as well as three housekeeping proteins and three negative controls. **(2)** They were simultaneously stained with three fluorescently-labeled antibodies to define the cellular-molecular compartments: macrophages by CD68; leukocytes by CD45; and tumor/kidney cells by pan-cytokeratin. **(3)** The slides were loaded onto the GeoMx DSP instrument and digitally scanned to produce fluorescent images of the cellular compartments for each spot, which were sequentially illuminated with ultraviolet light to cleave the oligonucleotides. **(4-6)** The oligonucleotides were collected by microcapillary aspiration and deposited into wells of a 96-well plate for the compartments of each spot. **(7)** They were then hybridized to four-color, six-spot optical barcodes and quantitated using the nCounter platform (NanoString Technologies).

Methods (continued)

Figure 2: Representative TMA spot

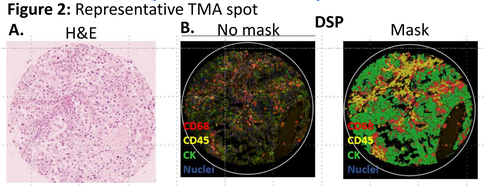

Figure 2. Images of a representative spot from the TMAs showing **(A)** hematoxylin and eosin staining and **(B)** the fluorescence patterns of the cellular-molecular compartment markers (left), and the compartment masks created by the GeoMx instrument for DSP (right).

Table 1: TMA descriptive statistics

	n (%) or median (95% confidence interval)		
	YTMA-84	YTMA-166	YTMA-528
Unique Patients	25	14	59
Unique Samples	50	28	95
Samples with replicate #:			
1	50 (100)	6 (21)	27 (28)
2	0 (0)	4 (14)	68 (72)
3	0 (0)	9 (32)	0 (0)
4	0 (0)	9 (32)	0 (0)
Matched pairs	25	14	24
Age, years (at sample date)	71.0 (62.0,76.0)	56.0 (50.0,69.0)	60.6 (57.9,62.8)
Male	15 (60)	9 (64)	46 (78)
Histology:			
ccRCC	22 (88)	-	87 (92)
nccRCC	3 (12)	-	8 (8)
IMDC score:			
Good	-	-	6 (13)
Intermediate	-	-	29 (64)
Poor	-	-	10 (22)
Nephrectomy	-	-	50 (85)
Primary tumor size (cm)	5.0 (3.5, 7.0)	6.5 (3.5, 10.7)	9.8 (8.0, 11.0)
Sample Location:			
Adjacent normal kidney	25 (50)	0 (0)	0 (0)
Primary	25 (50)	14 (50)	28 (29)
Metastatic - brain	0 (0)	0 (0)	24 (25)
Metastatic - lung	0 (0)	4 (14)	19 (20)
Metastatic - bone	0 (0)	2 (7)	15 (16)
Metastatic - other	0 (0)	8 (29)	9 (9)
Presence of *de novo* brain mets	-	-	12 (20)
Received IO therapy at some point	-	-	41 (69)

Results (continued)

Table 2: Multivariate Cox regression analysis

Characteristic	HR[1]	95% CI[1]	p-value
BCLXL	0.57	0.14, 2.28	0.4
BCL6	1.36	0.29, 6.43	0.7
STING	0.08	0.01, 0.39	<0.001
HLA.DR	8.80	0.65, 120	0.094
CD11c	1.36	0.20, 9.12	0.8
IMDC			0.023

Table 2. Univariate and multivariate Cox proportional hazards regression analyses of survival after brain metastasis occurrence was performed on the data from YTMA-528 for each compartment, using all 52 immuno-oncology markers, as well as IMDC score, tumor size, tumor grade, sex, age, and the presence of *de novo* brain metastases as inputs. Significant factors on univariate analysis were subjected to multivariate analysis. When looking at all tumor types together (primary tumors and metastases), on multivariate analysis, only IMDC score in all compartments, and fibronectin (HR 1.74, p=0.025) in the CK compartment remained significant. The analysis was repeated for marker expression levels in metastases and primary tumors separately. The results for the multivariate analysis of the CD45 compartment of primary tumors is shown above; among the other conditions, only fibronectin (HR 2.6, p=0.005) in the CK compartment of metastases was significant on multivariate analysis. Survival plots, and the corresponding HRs and log-rank p-values, based on dichotomized (by median) STING expression in the CD45 compartment and tumor type are shown in **Figure 5**.

Results

Figure 4: Unsupervised clustering of CD45 compartment

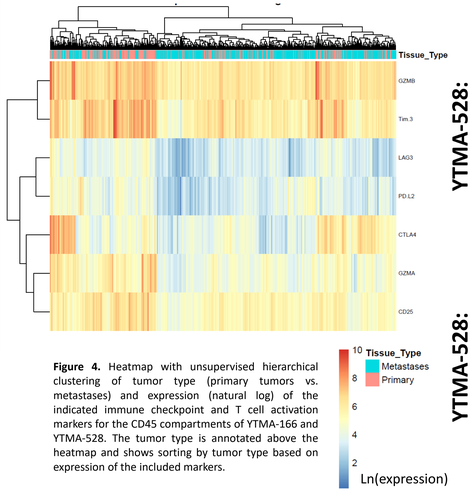

Figure 4. Heatmap with unsupervised hierarchical clustering of tumor type (primary tumors vs. metastases) and expression (natural log) of the indicated immune checkpoint and T cell activation markers for the CD45 compartments of YTMA-166 and YTMA-528. The tumor type is annotated above the heatmap and shows sorting by tumor type based on expression of the included markers.

Figure 5: Survival analysis, post-brain metastasis, by STING expression and tumor type in the CD45 compartment

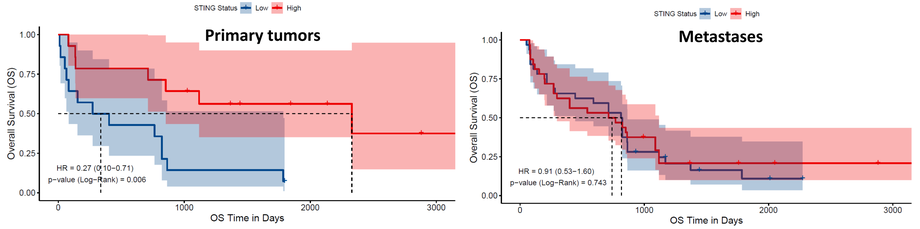

Figure 3: Volcano plots by compartment, TMA

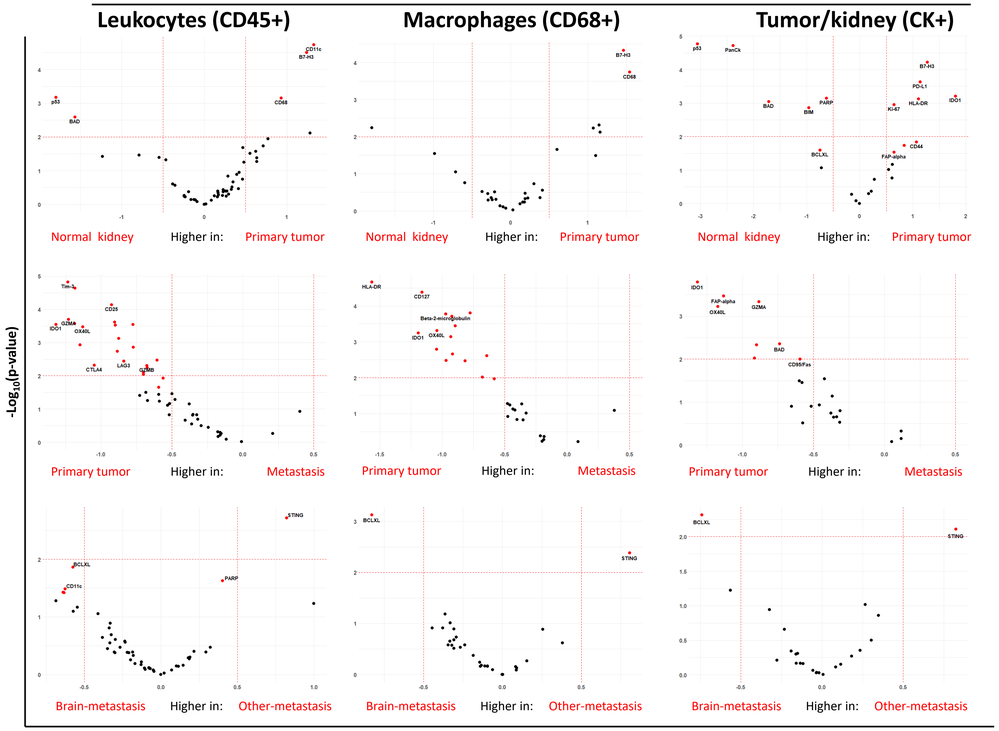

Figure 3. Volcano plots comparing the expression of immuno-oncology markers for the listed tissue types in each cellular compartment, with the $\log_2$(fold-change) on the x-axis and the $-\log_{10}$(p-value) on the y-axis. For the upper two rows, markers with an FDR < 0.05 are colored in red; for the bottom row, markers with a p < 0.05 are colored in red (exploratory). Select markers are labeled. Vertical dashed red lines indicate | $\log_2$(fold-change) | = 0.5, and the horizontal dashed red line indicates p=0.01, for comparison purposes across graphs. The TMA from which the data derives, and the tissue type comparison, is indicated on the left.

Conclusions

- DSP of progressively advanced stages of RCC, including brain metastases, revealed reduced levels of multiple immune checkpoints and T cell activation markers in metastases versus primary tumor samples, and higher inflammatory macrophage activation markers in primary samples.
- Brain metastases also had features distinct from metastases to other sites, including potentially higher levels of the anti-apoptotic BCL-XL, and lower levels of STING.
- STING expression in the leukocytes of primary tumors may have prognostic importance for patients who develop brain metastases – further validation is needed.
- As predictive biomarkers are developed for immunotherapy in RCC, consideration should be given to what anatomic sites the tumor samples are taken from.

Acknowledgements: The authors would like to acknowledge Lori Charette and Yale Pathology Tissue Services for help in constructing YTMA-528. This work was funded in part by NIH grants P50 CA121974 (M. Bosenberg and H. Kluger), R01 CA227472 (H. Kluger and K. Herold), R01 CA216846 (H. Kluger and G. Desir), and T32-CA233414-02 (D. Schoenfeld).